

MDPI

Article

1/f Additive Phase Noise Analysis for One-Port Injection-Locked Oscillators

Inwon Suh 1,20, Patrick Roblin 2,*0 and Youngseo Ko 2,3

- ¹ Broadcom, Irvine, CA 92618, USA
- Department of Electrical & Computer Engineering, The Ohio State University, Columbus, OH 43210, USA
- ³ Psemi, A Murata Company, San Diego, CA 92121, USA
- * Correspondence: roblin.1@osu.edu; Tel.: +1-(614)292-0998

Abstract: The 1/f additive phase noise of one-port injection-locked oscillators is experimentally characterized and analyzed using a simple analytic model based on the generalized 1/f Kurokawa theory. To experimentally verify the prediction of the simple analytic model proposed, two negative-conductance transmission line pHEMT oscillators operating at 2.4828 GHz and 2.485 GHz were designed and fabricated. A new configuration for integrating an additive phase noise measurement system with a large signal network analyzer (LSNA) is introduced to jointly acquire both the noise and RF waveforms of the one-port injection-locked oscillator. The Kurokawa derivatives needed for the analytic expression were experimentally obtained using the LSNA measurements and optimized to accurately model the corner frequency. A good agreement between the predicted and experimental results was obtained for both the injection-locked and free-running oscillators. In contrast to phase noise measurements of the free-running oscillator, which can only characterize the oscillator-upconverted $1/f^3$ noise, the additive phase noise characterization of the injection-locked oscillator is shown to provide the means to directly observe and characterize the input-referred intrinsic 1/f noise source of the oscillator negative resistance.

Keywords: additive phase noise measurement; injection locking; 1/f noise; oscillator



Citation: Suh, I.; Roblin, P.; Ko, Y. 1/f Additive Phase Noise Analysis for One-Port Injection-Locked Oscillators. *Electronics* **2023**, *12*, 264. https://doi.org/10.3390/electronics12020264

Academic Editor: Boris Andrievsky

Received: 11 November 2022 Revised: 13 December 2022 Accepted: 21 December 2022 Published: 4 January 2023



Copyright: © 2023 by the authors. Licensee MDPI, Basel, Switzerland. This article is an open access article distributed under the terms and conditions of the Creative Commons Attribution (CC BY) license (https://creativecommons.org/licenses/by/4.0/).

1. Introduction

Low-frequency 1/f noise is of significant importance in oscillator design since it generates a noise sideband with $1/\Delta f^3$ dependence when it is up-converted to the RF carrier signal [1]. The up-converted 1/f noise oscillator can then impact the performance of communication systems [2,3]. Among many approaches for reducing this detrimental near carrier noise, the injection-locking method has been effectively used for minimizing the phase noise of oscillators. An important body of work [4–10] is already available on the analysis of injection-locked oscillator phase noise. Previous analyses for *white* noise showed that the near carrier phase noise spectrum of the injection-locked oscillator follows that of the injection signal [4–8]. In this paper, we shall instead focus on using injection locking to characterize and model the intrinsic 1/f additive phase noised contributed by a negative resistance in an oscillator.

There have been continuous advances in microwave noise measurement systems [11]. The measurement of the additive phase noise in amplifiers can be realized using a differential testbed, which ideally cancels the noise in the external RF source [12–16]. These systems can be used to obtain the additive phase noise characteristic of amplifiers under large signal operation [14,16].

In this paper, an additive phase noise measurement system is used to (1) synchronize the oscillator using injection locking and (2) measure its additive phase noise. An analytic expression for the 1/f additive phase noise of injection-locked negative-conductance oscillators is also derived using the generalized Kurokawa theory [17,18]. Note that the

Electronics **2023**, 12, 264 2 of 12

applicability of the behavioral Kurokawa theory to accurately model both low- and high-Q free-running oscillators in the presence and absence of AM-to-PM noise has been investigated in detail in [18]. When injection locking is turned off, the analytic expression reported in this paper for the 1/f additive phase noise in phase-locked oscillators is verified to reduce to the 1/f phase noise analytic expression derived in [18] for the free-running oscillator. The new measurement and analysis techniques are then applied to two oscillators. A reasonable agreement for the phase noise level and the corner frequency is obtained between the measured and theoretical 1/f additive phase noise spectrum for the two injection-locked oscillators considered. To the knowledge of the authors, this is the first report to analyze the 1/f additive phase noise of an one-port injection-locked oscillator.

This paper is organized as follows. In Section 2, the 1/f additive phase noise analytic model for the injection-locked oscillator is derived using the Kurokawa theory. Section 3 introduces the new scheme used for the integration of the additive phase noise measurement setup with a large signal network analyzer (LSNA) as needed for this work. In Section 4, the new measurements developed for the Kurokawa model parameter extraction are presented. The analytic solution for the 1/f additive phase noise of the injection-locked oscillator is compared with experimental results in Section 5. Finally, the results obtained are summarized in Section 6.

2. 1/f Additive Phase Noise Model for Injection-Locked Oscillator

An admittance model for an injection-locked oscillator is shown in Figure 1. It is divided into a frequency- and amplitude-sensitive nonlinear active part $Y_{IN}(A,\omega)$, a frequency-sensitive linear passive part $Y_L(\omega)$, an 1/f noise current source I_N , and an injection-locking current source with amplitude $|I_S|$ and frequency ω_S . Note that ω_S was selected to be close to the self oscillation frequency ω_0 of the free-running oscillator. The voltage across the tank in Figure 1 can be written as:

$$\begin{split} v(t) &= \mathbf{Re} \Big[A(t) \ e^{j(\omega t + \phi(t))} \Big] + \text{harmonics} \\ \text{with } A(t) &= A_S + \delta A(t) \\ \omega &= \omega_S + \delta \omega(t) = \omega_S + \frac{d\phi(t)}{dt} - j \frac{1}{A(t)} \frac{dA(t)}{dt}. \end{split}$$

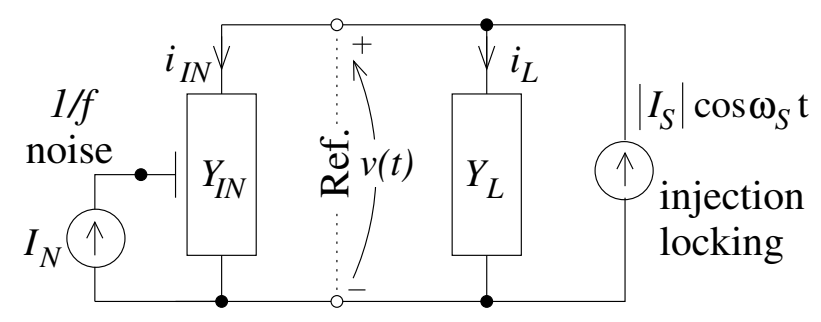


Figure 1. Admittance model for one-port injection-locked oscillator.

Performing a first-order Taylor series expansion of the total admittance ($Y_T = Y_{IN} + Y_L$) about the steady state injection-locked condition A_S , ω_S , and I_{N0} , we obtain for the current at the fundamental frequency ω_S :

$$|I_{S}|\cos \omega_{S}t$$

$$= \mathbf{Re} \Big\{ A(t)e^{j(\omega_{S}t + \phi(t))} [Y_{L}(\omega) + Y_{IN}(A, \omega, I_{N})] \Big\}$$

$$= \mathbf{Re} \Big\{ A(t)e^{j(\omega_{S}t + \phi(t))} [Y_{L,S} + Y_{IN,S} + Y'_{I,S} \delta \omega + Y'_{IN,S} \delta A + Y'_{IN,I,S} \delta I_{N}] \Big\}$$
(1)

Electronics **2023**, 12, 264 3 of 12

using the definitions $Y_{IN,S} = Y_{IN}(A_S, \omega_S, I_{N0})$, $Y_{L,S} = Y_L(\omega_S)$, $Y_x = G_x + iB_x$, and with the prime (') symbol standing for a derivative. The master Equation (1) can be divided into real and imaginary parts as follows:

$$G_{L,S} + G'_{T,S} \frac{d\phi(t)}{dt} + \frac{B'_{T,S}}{A_S} \frac{dA_S(t)}{dt} + G_{IN,S}$$

$$+ G'_{IN,S} \delta A(t) + G'_{IN,I,S} \delta I_N(t) = \frac{|I_S|}{A_S} \cos[\phi(t)], \qquad (2)$$

$$B_{L,S} + B'_{T,S} \frac{d\phi(t)}{dt} - \frac{G'_{T,S}}{A_S} \frac{dA_S(t)}{dt} + B_{IN,S}$$

$$+ B'_{IN,S} \delta A(t) + B'_{IN,I,S} \delta I_N(t) = -\frac{|I_S|}{A_S} \sin[\phi(t)]. \qquad (3)$$

Equation (3) for 1/f additive phase noise analysis in a one-port oscillator exhibits a similar structure to Equation (22) in [7] for the two-port oscillator and white noise sources. This similarity in the master equation structure suggests that the analysis technique used here for 1/f additive phase noise in one-port injection-locked oscillators can also be applied to two-port injection-locked oscillators.

In the frequency domain, for small phase perturbations $\phi = \phi_S + \delta \phi$, Equations (2) and (3) at the offset frequency Ω yield:

$$\mathbf{D} \begin{bmatrix} \delta A(\Omega) \\ \delta \phi(\Omega) \end{bmatrix} = \begin{bmatrix} -G'_{IN,I,S} \delta I_N(\Omega) \\ -B'_{IN,I,S} \delta I_N(\Omega) \end{bmatrix}$$
(4)

with
$$\mathbf{D} = \begin{bmatrix} G'_{IN,S} + j\Omega \frac{B'_{T,S}}{A_S} & \frac{|I_S|}{A_S} \sin \phi_S + j\Omega G'_{T,S} \\ B'_{IN,S} - j\Omega \frac{G'_{T,S}}{A_S} & \frac{|I_S|}{A_S} \cos \phi_S + j\Omega B'_{T,S} \end{bmatrix}$$
.

By taking the inverse, we obtain,

$$\begin{bmatrix} \delta A(\Omega) \\ \delta \phi(\Omega) \end{bmatrix} = \mathbf{D}^{-1} \begin{bmatrix} -G'_{IN,I,S} \, \delta I_N(\Omega) \\ -B'_{IN,I,S} \, \delta I_N(\Omega) \end{bmatrix}. \tag{5}$$

Focusing on phase noise, an analytic expression for the additive phase noise of an injection-locked oscillator perturbed by an N-C noise of spectral density $S_{I_N} = S/|\Omega|^{1+\epsilon}$ is obtained (see Appendix A for a detailed derivation):

$$S_{\phi,add}(\Omega) = S_{I_N}(\Omega) \times \left| \frac{\delta \phi(\Omega)}{\delta I_N(\Omega)} \right|^2$$

$$= \frac{S}{|\Omega|^{1+\epsilon}} \times \frac{C^2 A_S^2 + A^2 \Omega^2}{|I_S|^2 N^2 + Q\Omega^2 + |Y_T'|^4 \Omega^4}$$
(6)

Electronics **2023**, 12, 264 4 of 12

where, using $\mathbf{y}_S = [\cos(-\phi_S)\sin(-\phi_S)]$, we define:

$$C = G'_{IN,S}B'_{IN,I,S} - B'_{IN,S}G'_{IN,I,S} \equiv \frac{\partial \mathbf{Y}_{IN,S}}{\partial A} \times \frac{\partial \mathbf{Y}_{IN,S}}{\partial I_N}$$

$$A = G'_{T,S}G'_{IN,I,S} + B'_{T,S}B'_{IN,I,S} \equiv \frac{\partial \mathbf{Y}_{T,S}}{\partial \omega} \cdot \frac{\partial \mathbf{Y}_{IN,S}}{\partial I_N}$$

$$B = G'_{T,S}B'_{IN,I,S} - B'_{T,S}G'_{IN,I,S} \equiv \frac{\partial \mathbf{Y}_{T,S}}{\partial \omega} \times \frac{\partial \mathbf{Y}_{IN,S}}{\partial I_N}$$

$$\alpha = G'_{IN,S}G'_{T,S} + B'_{IN,S}B'_{T,S} \equiv \frac{\partial \mathbf{Y}_{IN,S}}{\partial A} \cdot \frac{\partial \mathbf{Y}_{T,S}}{\partial \omega}$$

$$\beta = G'_{IN,S}B'_{T,S} - B'_{IN,S}G'_{T,S} \equiv \frac{\partial \mathbf{Y}_{IN,S}}{\partial A} \times \frac{\partial \mathbf{Y}_{T,S}}{\partial \omega}$$

$$N = \cos(\phi_S)G'_{IN,S} - \sin(\phi_S)B'_{IN,S} \equiv \mathbf{y}_S \cdot \frac{\partial \mathbf{Y}_{IN,S}}{\partial A}$$

$$P = \cos(\phi_S)B'_{T,S} + \sin(\phi_S)G'_{T,S} \equiv \mathbf{y}_S \times \frac{\partial \mathbf{Y}_{T,S}}{\partial \omega}$$

$$Q = A_S^2\beta^2 - 2|I_S|N|Y'_T|^2 + |I_S|^2P^2/A_S^2 + 2\beta|I_S|P.$$

Note that the obtained 1/f additive phase noise analytic expression in (6) for the injection-locked oscillator becomes the 1/f phase noise analytic expression Equation (14) in [18] when the injection-locking current source $|I_S|$ is neglected. Note also that the Ω^2 numerator and Ω^4 denominator terms in (6) can usually be neglected. The resulting simplified equation is:

$$S_{\phi,add}(\Omega) \simeq \frac{S}{|\Omega|^{1+\epsilon}} \times \frac{C^2 A_S^2}{|I_S|^2 N^2 + Q\Omega^2}.$$
 (7)

Then, using (7), a simplified analytic expression for the corner frequency Ω_c can be obtained:

$$\Omega_c = \sqrt{|I_S|^2 N^2 / Q} \tag{8}$$

It is to be noted that, within the locking bandwidth (below the corner frequency Ω_c), the additive phase noise $S_{\phi,add}$ is directly proportional to the intrinsic N-C noise spectrum S_{I_N} .

3. Measurement System Description

Figure 2 shows a previous additive noise measurement setup, which was reported in [19]. The advantage of the additive phase noise measurement system is that it ideally cancels the noise of the locking RF signal source in the system and enables us to measure the intrinsic noise of the negative conductance in the injection-locked oscillator. However, this setup was developed for two-port injection-locked oscillators. It was subsequently found that this two-port method was not accurate for characterizing one-port injection-locked oscillators. Indeed, in the two-port measurement system, the incident and reflected waves at the one-port oscillator port are recovered by de-embedding from the two-port large-signal measurements the output signal of the three port-circulator, and this was found to not yield sufficiently accurate and consistent data. The new improved additive phase noise measurement system proposed in Figure 3 for a one-port oscillator has the advantage of directly measuring at Port 2 the incident a_2 and reflected b_2 waves of the oscillator and, thus, does not require any de-embedding. Note also that the LSNA coupler provides a few dB of attenuation, which further improves the matching between the circulator and the oscillator. Additional padding can be introduced if needed.

Electronics **2023**, 12, 264 5 of 12

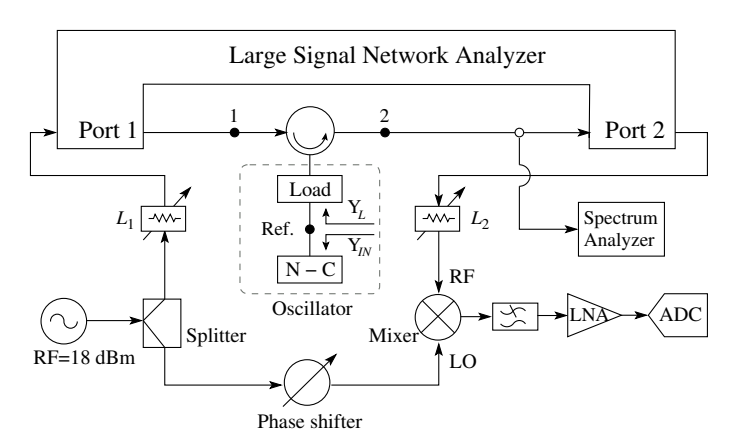


Figure 2. Previous additive phase noise measurement system in [19] integrated with an LSNA for a two-port injection-locked oscillator. N-C stands for the negative-conductance circuit.

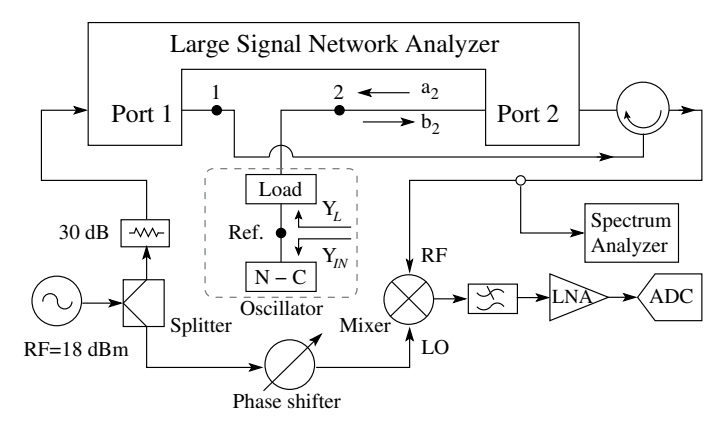


Figure 3. New additive phase noise measurement system integrated with an LSNA for a one-port injection-locked oscillator with a negative-conductance (N-C) circuit.

The LSNA is used to measure the amplitude and phase of the incident locking signal at Port 1, and the incident and reflected waves of the injection-locked oscillator at Port 2. Port 1 is used to accurately monitor the power of the injection signal and, thus, facilitates reproducing the injection locking measurements in various successive measurements. Note that a circulator is used for the signal injection in the oscillator. A phase shifter is used to maintain a quadrature condition between the RF and LO port of the mixer for measuring the additive phase noise of the injection-locked oscillator. A picture of the testbed is shown in Figure 4.



Figure 4. Testbed used for the measurement of additive phase noise.

The oscillator circuit tested is an *Avago* ATF54143 pHEMT negative-conductance oscillator fabricated on the RF/Duroid 5880 substrate ($\epsilon_r = 2.2$ and h = 45 mil). Note

Electronics **2023**, 12, 264 6 of 12

that the oscillator circuit is divided into two separate circuit boards composed of the negative-conductance active circuit and the passive load circuit, respectively. Figure 5 depicts the simplified schematic of the active circuit designed and fabricated. In this work, two different load circuits with different DC biasing are used, respectively, to test the theory with the measurements for two different operating conditions. The simplified schematic of each passive load circuit is shown in Figures 6 and 7, respectively.

Since the LSNA measures the incident and reflected waves at Port 2 in Figure 3, the scattering parameters of the passive load circuit are used to shift the measurement reference plane from Port 2 to the negative-conductance circuit reference plane noted "Ref.". This permits us to extract the phase ϕ_S of the voltage v(t) relative to the injection-locking current. For the DC biasing, $V_{GS}=0.55$ V and $V_{DS}=2.00$ V yielding I_{DS} of 24 mA are used for the first oscillator, while $V_{GS}=0.65$ V and $V_{DS}=1.18$ V yielding I_{DS} of 21 mA are used for the second oscillator, respectively. A spectrum analyzer (*Agilent* E4405B with the phase noise option) is also used to measure the phase noise of the free-running oscillator when the locking RF signal source is turned off.

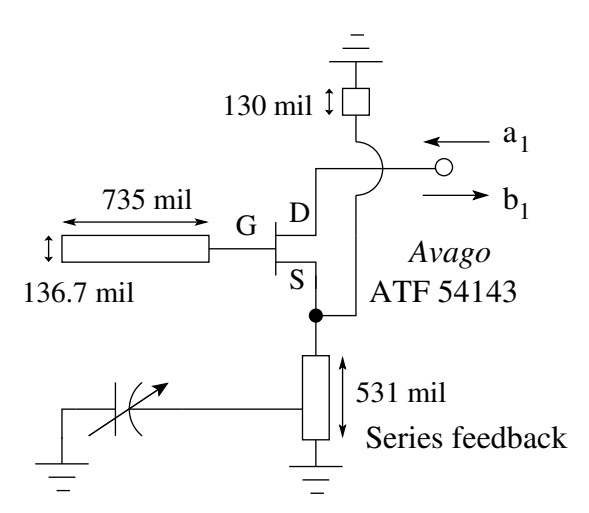


Figure 5. Schematic of the negative-conductance active circuit. The width of all the microstrip lines is 136.7 mil. RT/Duroid 5880 with ε_r = 2.2 and thickness h = 45 mil is used for the substrate.

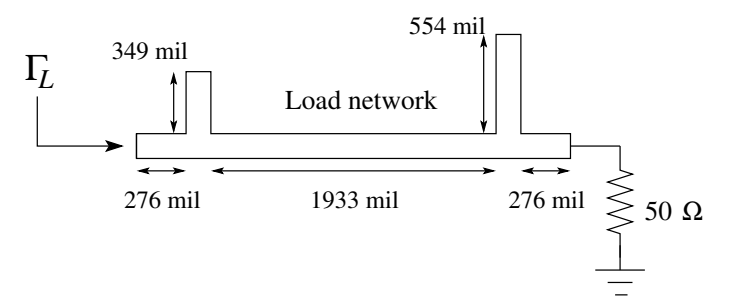


Figure 6. Schematic of the first passive load circuit (Load Circuit 1). The width of all the microstrip lines is 136.7 mil.

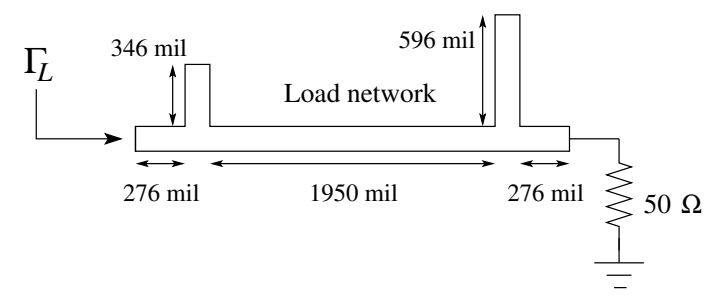


Figure 7. Schematic of the second passive load circuit (Load Circuit 2). The width of all the microstrip lines is 136.7 mil.

Electronics **2023**, 12, 264 7 of 12

4. Experimental Model Parameter Extraction

In this work, the model parameter extraction was performed experimentally using both small- and large-signal measurements. The four required parameters, $G'_{IN,S}$, $B'_{IN,S}$, $G'_{T,S}$, and $B'_{T,S}$ in (6), were measured experimentally at the operating point (A_S , ω_S).

4.1. $G'_{IN,S}$ and $B'_{IN,S}$ Extraction

First, the two parameters $G'_{IN,S}$ and $B'_{IN,S}$ were extracted by measuring the admittance of the active device in Figure 5 for several power levels near the operating amplitude A_S at the injection-locked frequency f_S . Figure 8 shows the LSNA measurement result of the output power versus the input drive level a_1 . As shown, the incident wave a_1 is swept from -26 dBm to 12 dBm at the injection-locked frequency f_S . The black dot represents the operating amplitude A_S used for the $G'_{IN,S}$ and $B'_{IN,S}$ extraction. Note that a 0.1 dB power sweep step was used near the operating amplitude A_S to increase the accuracy level of the derivative extraction. A least-squares fit was further used to remove any residual numerical noise.

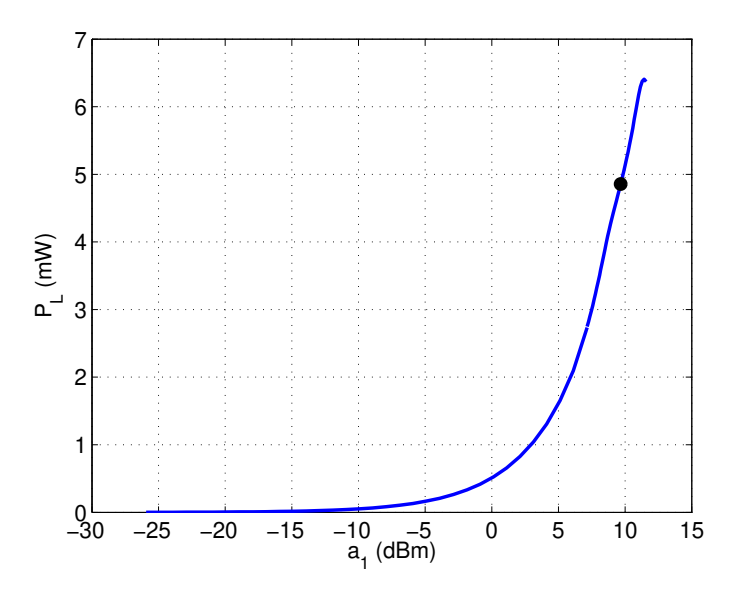


Figure 8. Output power sweep result of the active circuit in Figure 5 using the LSNA at the frequency f_S . The black dot indicates the operating amplitude A_S used for $G'_{IN,S}$ and $B'_{IN,S}$ extraction.

4.2. $G'_{T,S}$ and $B'_{T,S}$ Extraction

The frequency-dependent parameters $G'_{T,S}$ and $B'_{T,S}$ were obtained by adding $\partial G_{IN,S}/\partial \omega$ and $\partial B_{IN,S}/\partial \omega$ to $G'_{L,S}$ and $B'_{L,S}$, respectively.

$$G'_{T,S} = \frac{\partial G_{IN,S}}{\partial \omega} + G'_{L,S}$$
$$B'_{T,S} = \frac{\partial B_{IN,S}}{\partial \omega} + B'_{L,S}$$

To extract $\partial G_{IN,S}/\partial \omega$ and $\partial B_{IN,S}/\partial \omega$, a 13-tone frequency-modulated (FM) signal equally spaced with 100 kHz is injected into the active device in Figure 5 using the ESG source. The FM signal thus synthesized maintains the desired constant oscillation amplitude A_S while modulating the frequency around f_S . Then, the input reflection coefficients are obtained using (9).

$$\Gamma_{IN}(n\omega_S, t) = \frac{\sum_{p=-SSB}^{SSB} b_1(n\omega_S + p\Delta\omega)e^{jp\Delta\omega t}}{\sum_{p=-SSB}^{SSB} a_1(n\omega_S + p\Delta\omega)e^{jp\Delta\omega t}}$$
(9)

Electronics **2023**, 12, 264 8 of 12

This time domain approach for obtaining the input reflection coefficients at the fundamental and harmonic frequencies is explained in detail in [20]. This approach provides a convenient and accurate way to obtain $\partial G_{IN,S}/\partial \omega$ and $\partial B_{IN,S}/\partial \omega$. Note that a frequency offset ($\Delta \omega$) of about 100 kHz and 20 single sideband (SSB) tones were used for this LSNA measurement.

A network analyzer was used to measure the admittance of the load circuit near the injection-locked frequency of f_S for extracting $G'_{L,S}$ and $B'_{L,S}$. A 1 MHz frequency spacing was used together with a least-squares fit to remove any residual numerical noise. Note that the total frequency-dependent parameters $G'_{T,S}$ and $B'_{T,S}$ are further optimized to accurately predict the corner frequency (8) in the Experimental Results Section presented next.

5. Experimental Results

The comparison of the phase noise results of the oscillator with the Load Circuits 1 and 2 is shown in Figures 9 and 10, respectively. The additive phase noise spectrum of the injection-locked oscillator was measured seven times with the new measurement system in Figure 3, and the average value is plotted (red solid curve) to reduce the measurement noise. Plotted as well are the phase noise spectra measured for the free-running (green solid line) and injection-locked (blue solid line) oscillators using a spectrum analyzer, the *Agilent* E4405B, with the phase noise option. Note that the *additive* phase noise of the two injection-locked oscillators has a slope of $1/f^{0.90}$ and $1/f^{0.68}$, respectively, due to the rejection of the noise up-conversion within the locking bandwidth, while the phase noise of the free-running oscillators has a slope of $1/f^{2.90}$ and $1/f^{2.68}$, respectively, due to the 1/f noise up-conversion. For frequencies above the locking bandwidth, the additive phase noise and phase noise for the injection-locked oscillators are seen to be the same as the phase noise of the free-running oscillators. However, the noise within the locking bandwidth contributes the dominant portion of the oscillator phase noise in both the free-running and injection-locked oscillators.

In order to predict the 1/f additive phase noise spectrum of the injection-locked oscillator (red solid line) in Figures 9 and 10 using (6), a three-parameter ($G'_{IN,I,S}$, $B'_{IN,I,S}$, and S) fitting approach was first used. Since the origin and location of the 1/f noise sources in the device is unknown, this fitting is needed to obtain the three input-referred 1/f noise parameters ($G'_{IN,I,S}$, $B'_{IN,I,S}$, and S) in the final 1/f phase noise expression in (6). Note that the measured Kurokawa parameters ($G'_{IN,S}$, $B'_{IN,S}$, $G'_{I,S}$, and $B'_{I,S}$) from the previous section were directly used for this fitting. As a result, a 0.1 dB difference in the 1/f additive phase noise level was observed for both oscillators with this fitting approach. This result clearly indicates that the intrinsic noise source of the injection-locked oscillator can be extracted using this three-1/f noise parameter-fitting approach. However, the corner frequency Ω_c of the additive phase noise was not well predicted.

To further optimize the corner frequency of the 1/f additive phase noise in (8), it was found to be necessary to also optimize the two previously experimentally obtained $G'_{T,S}$ and $B'_{T,S}$ parameters beside the three noise parameters. Thus, a total of five fitting parameters is needed for accurate modeling. Note that the initially obtained three-1/f parameters ($G'_{IN,I,S}$, $B'_{IN,I,S}$, and S) remained about the same for this five-parameter fitting. The black dashed line in Figures 9 and 10 shows the final results, which accurately fit both the 1/f additive phase noise spectrum and the corner frequency (black dot).

To validate the modified parameter extraction and fitting approach used, the phase noise of the free-running oscillator predicted by the generalized Kurokawa theory [17,18] was calculated using the *same* extracted parameters. As shown in Figures 9 and 10, the modeled curve (blue dashed-dotted line) predicts fairly well the experimental phase noise spectrum of the free-running oscillator (green solid lines). This additional prediction of the phase noise of the free-running oscillator provides some additional confidence in the application of the extracted Kurokawa parameters to the injection-locking analysis. Note that, when suppressing the injection-locking current source $|I_S|$ in (6), the 1/f additive phase noise analytic expression for the injection-locked oscillator reduces then to that of

Electronics 2023, 12, 264 9 of 12

the 1/f phase noise analytic expression Equation (14) in [18]. This can easily be verified using the identity:

 $C|Y_T'|^2 = \alpha \mathcal{B} + \beta \mathcal{A}.$

This theoretical link and the experimental verification in Figure 9 and 10 indicates that the methodology presented here is useful for determining the intrinsic phase noise of negative resistance oscillators both with and without injection locking.

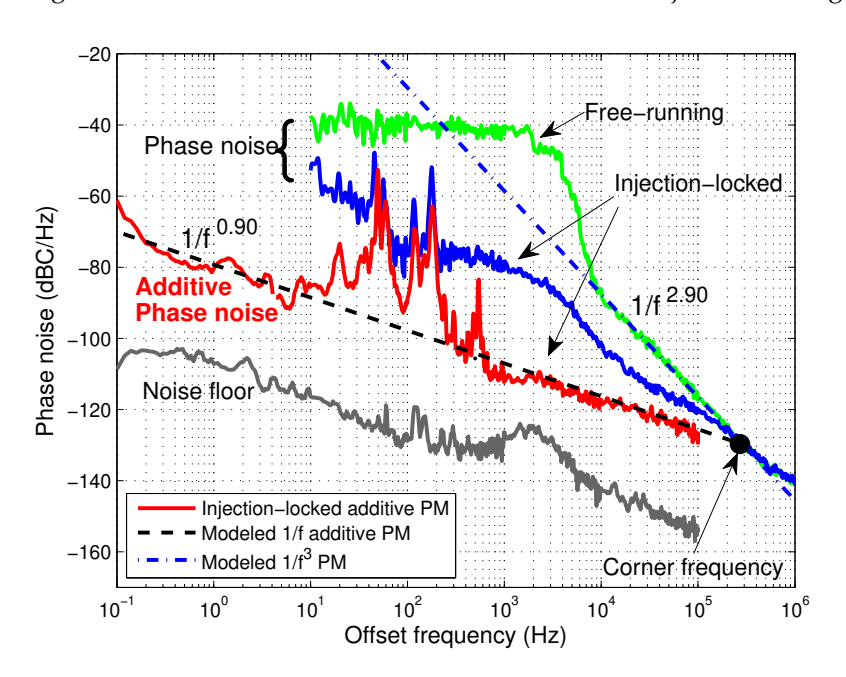


Figure 9. Comparison of additive phase noise $S_{\phi,add}$ and phase noise S_{ϕ} for the pHEMT oscillator with Load Circuit 1 operating at 2.4828 GHz.

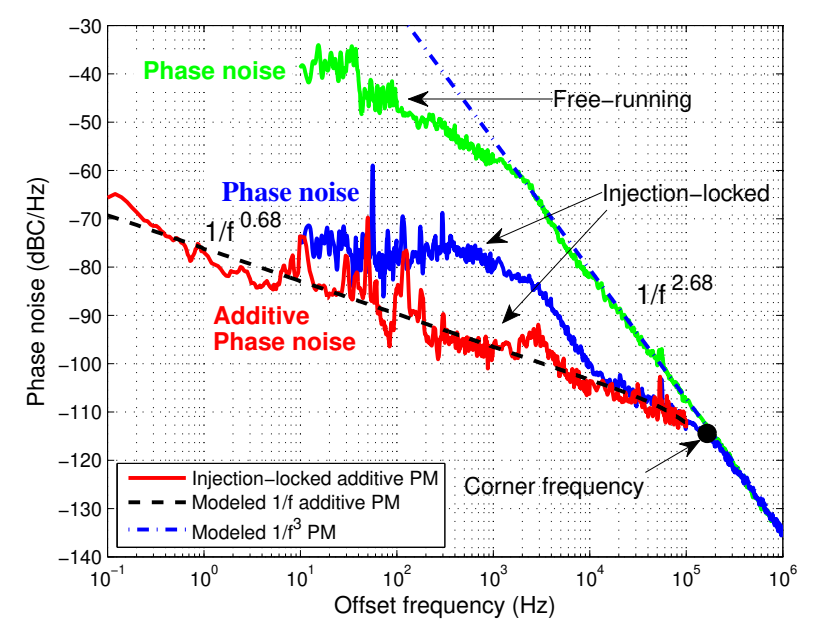


Figure 10. Comparison of additive phase noise $S_{\phi,add}$ and phase noise S_{ϕ} for the pHEMT oscillator with Load Circuit 2 operating at 2.485 GHz.

6. Conclusions

In this paper, an 1/f additive phase noise analysis for one-port injection-locked oscillators was presented to characterize their additive phase noise. An analytic expression for the 1/f additive phase noise of the injection-locked oscillator was derived using the

Electronics 2023, 12, 264 10 of 12

generalized Kurokawa theory. A new additive phase noise measurement system integrated with an LSNA was developed to measure the 1/f additive phase noise for one-port injection-locked oscillator, as well as the amplitude and phase of the locked oscillation. The Kurokawa derivatives needed by the theory were experimentally extracted using smalland large-signal measurements. The three unknown noise parameters (S and $Y'_{IN,L,S}$) were then extracted to fit the additive phase noise. To accurately predict the corner frequency, it was found necessary to optimize $\mathbf{Y}'_{T.S}$. Besides fitting the 1/f additive phase noise results for injection-locked operation well, the obtained analytic solution was verified to predict the experimental phase noise results for two different free-running pHEMT microstrip line oscillators well. Note that the extraction method applied in this paper is not fully predictive due to the fact that, overall, five fitting parameters had to be used. This certainly points to the limitation of the simple circuit model in Figure 1, which only relies on a single 1/fnoise source. However, the proposed Kurokawa analysis provides overall a reasonable and simple model for analyzing the experimental data for both the injection-locked and freerunning oscillators. The additive phase noise characterization measurements combined with injection locking and the extended Kurokawa analysis techniques described in this paper provides, thus, a useful technique for estimating the intrinsic 1/f noise source of negative resistance oscillators.

Author Contributions: Investigation, I.S. and Y.K.; Supervision, P.R. All authors have read and agreed to the published version of the manuscript.

Funding: This work was supported in part by the National Science Foundation (NSF) under Grant ECS 1129013.

Data Availability Statement: No data available.

Acknowledgments: The authors are indebted to Zoya Popović for insightful suggestions for improving the manuscript.

Conflicts of Interest: The authors declare no conflict of interest

Appendix A. Equation (6) Final Derivation

The system given by Equation (4):

$$A\delta + B\delta\phi = x$$
$$C\delta + D\delta\phi = y$$

with

$$x = -G'_{IN,I,S} \, \delta I_N(\Omega)$$

$$y = -B'_{IN,I,S} \, \delta I_N(\Omega)$$

$$A = a + j\alpha = G'_{IN,S} + j\Omega \frac{B'_{T,S}}{A_S}$$

$$B = b + j\beta = \frac{|I_S|}{A_S} \sin \phi_S + j\Omega G'_{T,S}$$

$$C = c + j\gamma = B'_{IN,S} - j\Omega \frac{G'_{T,S}}{A_S}$$

$$D = d + j\delta = \frac{|I_S|}{A_S} \cos \phi_S + j\Omega B'_{T,S}$$

admits for solution:

$$\delta \phi = \frac{Cx - Ay}{BC - AD} = \frac{s + j\sigma}{r + j\rho}$$

Electronics **2023**, 12, 264

with

$$r = bc - \beta\gamma - ad + \alpha\delta$$

$$\rho = \beta c + b\gamma - \alpha d - a\delta$$

$$s = xc - ya$$

$$\sigma = x\gamma - y\alpha$$

It results that we have:

$$\rho = \Omega \left[G'_{T} B'_{IN} - \frac{|I_{S}|}{A_{S}} \sin \phi \frac{G'_{T}}{A_{S}} - \frac{|I_{S}|}{A_{S}} \cos \phi \frac{B'_{T}}{A_{S}} - B'_{T} G'_{IN} \right]$$

$$= \Omega \left[-\beta - \frac{|I_{S}|}{A_{S}^{2}} P \right]$$

$$r = \frac{|I_{S}|}{A_{S}} \sin \phi B'_{IN} + \Omega^{2} \frac{G'_{T}^{2}}{A_{S}} - \frac{|I_{S}|}{A_{S}} \cos \phi G'_{IN} + \Omega^{2} \frac{B'_{T}^{2}}{A_{S}}$$

$$= -\frac{|I_{S}|}{A_{S}} N + \Omega^{2} \frac{|Y'_{T}|^{2}}{A_{S}}$$

$$s = -\delta I_{N} \left[G'_{IN,I} B'_{IN} - B'_{IN,I} G'_{IN} \right]$$

$$= -\delta I_{N} R$$

$$\sigma = -\delta I_{N} \left[G'_{IN,i} (-\Omega) \frac{G'_{T}}{A_{S}} - B'_{IN,i} \Omega \frac{B'_{T}}{A_{S}} \right]$$

$$= \delta I_{N} \frac{A}{A_{S}} \Omega$$

The final solution is then:

$$|\delta\phi|^2 = \frac{s^2 + \sigma^2}{r^2 + \rho^2}$$

with

$$s^{2} + \sigma^{2} = |\delta I_{N}|^{2} \left(R^{2} + \frac{A^{2}}{A_{S}^{2}} \Omega^{2} \right)$$

$$\rho^{2} = \Omega^{2} \left[\beta^{2} + \frac{|I_{S}|^{2}}{A_{S}^{4}} P^{2} + 2\beta \frac{|I_{S}|}{A_{S}^{2}} P \right]$$

$$r^{2} = \left[\frac{|I_{S}|^{2}}{A_{S}^{2}} N^{2} + \Omega^{4} \frac{|Y'_{T}|^{4}}{A_{S}^{2}} - 2\frac{|I_{S}|}{A_{S}^{2}} N|Y'_{T}|^{2} \Omega^{2} \right]$$

$$r^{2} + \rho^{2} = \left[\frac{|I_{S}|^{2}}{A_{S}^{2}} N^{2} + \Omega^{2} \left(\beta^{2} - 2\frac{|I_{S}|}{A_{S}^{2}} N|Y'_{T}|^{2} + \frac{|I_{S}|^{2}}{A_{S}^{4}} P^{2} + 2\beta \frac{|I_{S}|}{A_{S}^{2}} P \right) + \Omega^{4} \frac{|Y'_{T}|^{4}}{A_{S}^{2}} \right]$$

References

- 1. Siweris, H.J.; Schiek, B. Analysis of noise upconversion in microwave FET oscillators. *IEEE Trans. Microw. Theory Technol.* **1985**, 33, 233–242. [CrossRef]
- 2. Georgiadis, A. AC-coupling and 1/f Noise Effecs on Baseband OFDM Signals. *IEEE Trans. Commun.* **2006**, *54*, 1806–1814. [CrossRef]
- 3. Khanzadi, M.R.; Kuylenstierna, D.; Panahi, A.; Eriksson, T.; Zirath, H. Calculation of the Performance of Communication Systems From Measured Oscillator Phase Noise. *IEEE Trans. Circuits Syst. I* **2014**, *61*, 1553–1565. [CrossRef]
- 4. Chang, H.-C.; Cao, X.; Vaughan, M.J.; Mishra, U.K.; York, R.A. Phase noise in externally injection-locked oscillator arrays. *IEEE Trans. Microw. Theory Technol.* **1997**, 45, 2035–2042. [CrossRef]
- 5. Kurokawa, K. Injection locking of microwave solid-state oscillators. *Proc. IEEE* 1973, 61, 1386–1410. [CrossRef]

Electronics **2023**, 12, 264

- 6. Kurokawa, K. Noise in synchronized oscillators. IEEE Trans. Microw. Theory Technol. 1968, 16, 234–240. [CrossRef]
- 7. Ramírez, F.; Pontón, M.; Sancho, S.; Suárez, A. Phase-Noise Analysis of Injection-Locked Oscillators and Analog Frequency Dividers. *IEEE Trans. Microw. Theory Technol.* **2008**, *56*, 393–407. [CrossRef]
- 8. Suarez, A. Analysis and Design of Autonomous Microwave Circuits; John Wiley and Sons: Hoboken, NJ, USA, 2009.
- 9. Yabe, Y.; Tanaka, Hi.; Sekiya, H.; Nakagawa, M.; Mori, F.; Utsunomiya, K.; Keida, A. Locking Range Maximization in Injection-Locked Class-E Oscillator—A Case Study for Optimizing Synchronizability. *IEEE Trans. Circuits Syst. I* 2020, 67, 1762–1774. [CrossRef]
- Ardila, V.; Ramirez, F.; Suarez, A. Nonlinear Analysis of an Injection-Locked Oscillator Coupled to an External Resonator. IEEE Microw. Wirel. Compon. Lett. 2022, 32, 740–743. [CrossRef]
- 11. Wiatr, W.; Mercha, A.; Crupi, G.; Caddemi, A.; Schreurs, D.M. Source-Pull Characterization of FinFET Noise. In Proceedings of the MIXDES 2010, 17th International Conference on Mixed Design of Integrated Circuits and Systems, Wroclaw, Poland, 24–26 June 2010.
- 12. Montress, G.K.; Parker, T.E.; Loboda, M.J. Residual phase noise measurements of VHF, UHF, and microwave components. *IEEE Trans. Ultrason. Ferroelectr. Freq. Control* **1994**, *41*, 664–679. [CrossRef]
- Breitbarth, J.; Koebel, J. Additive (Residual) Phase Noise Measurement of Amplifiers, Frequency Dividers and Frequency Multipliers. Available online: https://www.microwavejournal.com/articles/6353-additive-residual-phase-noise-measurement-of-amplifiers-frequency-dividers-and-frequency-multipliers (accessed on 15 December 2022)
- 14. Janković, M.; Breitbarth, J.; Brannon, A.; Popović, Z. Measuring transistor large-signal noise figure for low-power and low phase noise oscillator design. *IEEE Trans. Microw. Theory Technol.* **2008**, *56*, 1511–1515. [CrossRef]
- 15. Rudolph, M.; Bonani, F. Low-frequency noise in nonlinear systems. IEEE Microw. Mag. 2009, 10, 84–92. [CrossRef]
- 16. Suh, I.; Roblin, P.; Ko, Y.; Yang, C.-K.; Malonis, A.; Arehart, A.; Ringel, S.; Poblenz, C.; Yi, P.; Speck, J.; et al. Additive phase noise measurement of AlGaN/GaN HEMTs using a large signal network analyzer and a tunable monochromatic light source. In Proceedings of the 2009 74th ARFTG Microwave Measurement Conference, Broomfield, CO, USA, 30 November–4 December 2009.
- 17. Mukherjee, J.; Roblin, P.; Akhtar, S. An analytic circuit-based model for white and flicker phase noise in LC oscillators. *IEEE Trans. Circuits Syst. I* **2007**, *54*, 1584–1598. [CrossRef]
- Suh, I.; Roblin, P. Model Comparison for 1/f Noise in Oscillators With and Without AM to PM Noise Conversion. IEEE Trans. Microw. Theory Technol. 2011, 59, 3129–3145. [CrossRef]
- 19. Roblin, P. Nonlinear RF Circuits and Nonlinear Vector Network Analyzers; Cambridge University Press: NY, USA, 2011.
- 20. Cui, X.; Doo, S.J.; Roblin, P.; Jessen, G.H.; Rojas, R.G.; Strahler, J. Real-time active loadpull of the 2nd & 3rd harmonics for interactive design of non-linear power amplifiers. In Proceedings of the 2006 68th ARFTG Conference: Microwave Measurement, Broomfield, CO, USA, 28 November–1 December 2006.

Disclaimer/Publisher's Note: The statements, opinions and data contained in all publications are solely those of the individual author(s) and contributor(s) and not of MDPI and/or the editor(s). MDPI and/or the editor(s) disclaim responsibility for any injury to people or property resulting from any ideas, methods, instructions or products referred to in the content.